IOP Conf. Series: Materials Science and Engineering **202** (2017) 012074 doi:10.1088/1757-899X/202/1/012074

Effect of Precursor Concentration Ratio on The Crystal Structure, Morphology, and Band Gap of ZnO Nanorods

A Fuad[1,2], A A Fibriyanti[1], Subakti[1,2], N Mufti[1,2] and A Taufiq[1,2]

[1]Department of Physics, Faculty of Mathematics and Natural Sciences, State University of Malang (Universitas Negeri Malang), Jl. Semarang No 5 Malang, Indonesia 65145
[2]Research Center for Minerals and Advanced Materials, State University of Malang (Universitas Negeri Malang), Jl. Semarang No 5 Malang, Indonesia 65145

Email: abdulloh.fuad.fmipa@um.ac.id

Abstract: In this present study, the ZnO nanorods were synthesized by using the hydrothermal method with various precursor concentrations. The ZnO nanorods were characterized by X-Ray Diffractometer (XRD) to identify the crystal structure, Scanning Electron Microscopy (SEM) to determine the morphology, and UV-Vis Spectrophotometer to determine the band gap. It was shown that the ZnO nanorods have hexagonal wurtzite crystal structure with the c-axis orientation at (002) Bragg's plane. The morphology of the ZnO particles was in a rod structure growing over the surface of the substrate. The diameter of the ZnO nanorods resulted ifrom the concentrations of 30, 35 mM, and 45 mM were 94.2, 156.3, and 76.7 nm, respectively. The data analysis of the UV-Vis data showed that the band gap of ZnO nanorods (~3.18 eV) was smaller than that of ZnO nanoparticles (~3.46 eV).

Keywords: ZnO, nanorod, crystal structure, band gap, solar cell.

1. Introduction

Electrical energy has a major role in supporting the national development. In term of the total use of electrical power, its growth rate was approximately 8.3 % annually from 222 TWh in 2015 becomes 305 TWh in 2019 [1]. Thereby, the availability of fossil as the primary source of energy in the world gradually reduces, so the development of the alternative electrical power including renewable energy should be conducted continually. In the last five years, solar cells with active material combined with halide organic/inorganic material and perovskite structure have caught many researchers' attention due to their ability in developing great power photovoltaic tools with high efficiency of up to 19.3 % [2].

Efficiency is influenced by the design of a solar cell involving the optimization of the layer structure, the characteristic of every layer like semiconductor layer, and the equipment parameter comprising a lifetime of charge carrier, the diffusion coefficient of minority charge carrier, and the surface recombination rate [3]. The level of exciton-dissociation efficiency and the charge carrier rate are definitely influenced by the surface morphology. The surface morphology of the active layer is one of the important factors affecting the efficiency of the hybrid solar cell.

ZnO is a semiconductor with the type-n of II-VI class with the bandgap of about 3.37 eV and excitonic bound energy of about 60 meV at room temperature [4]. On the other side, ZnO is categorized as a transparent conducting oxide material which is low-cost, looks promising, and it has been applied in many commercial applications such as light-emitting diode [5], UV sensor [6], nanolaser [7], gas sensor [8], and solar cell [9].

In semiconductor nanostructure material, one-dimension (1D) ZnO nanostructure can be modified into nanowires [10], nanobelts [11], and nanorods [12]. Each structure modification has a different physical characteristic. Nanorods structure, for example, can influence particular material to enhance its light absorption ability regarding its higher surface area [13]. In general, the fabrication of ZnO

nanostructures can be done by using thin film techniques such as spray pyrolysis, sputtering, MOCVD, and hydrothermal method [14]. The hydrothermal method has been widely used in producing the transparent oxide by using a simple, safe and low-cost technique [15].

In this research, the ZnO particles were modified to form nanorods initiated through the process of making the ZnO nanoparticle layered on an Indium Tin Oxide (ITO) substrate. In this work, the effect of precursor concentration on the crystal structure, morphology, and band gap of the ZnO nanorods is discussed.

2. Experimental Method

ITO was dipped into acetone in the ultrasonic cleaner for ten minutes and followed by the cleaning process using water before being dried by using a blower. Zinc acetate dehydrate (ZnAc) was dissolved in the ethanol and stirred by using a magnetic stirrer for 45 minutes. The PH of the solution was varied from 6 to 7. Furthermore, the ZnAc was mixed with MEA with the composition of 1:1 molar. The clean ITO substrate was placed on the spin coater holder by dropping the solution on the glass surface at the rotational speed of 3000 rpm. Preheating process was then conducted at 150 ^{o}C for 10 minutes followed by the annealing process at 550 ^{o}C for 2 hours. The solution was prepared by using the precursors of $Zn(NO_3)_2.4H_2O$ and hexamethylenetetramine/HMT in the water. Precursor concentrations used were 30, 35, and 45 mM with the molar comparison between Zn $(NO_3)_2.4H_2O$ and HMT of 1:1. The solution was then stirred at room temperature. Furthermore, the ZnO nanoparticles were dipped into the prepared solution. During the growing process, the solution was heated at a temperature of 90 °C for 6 hours. Water was used to clean the remaining salt from the sample surface. The obtained sample was then dried by using a mini electric blower. Lastly, the ZnO nanorods on the ITO substrate were annealed at a temperature of 550 ^{o}C for 2 hours. The samples were characterized by using X-Ray Diffractometer (XRD), Scanning Electron Microscopy (SEM), and UV-Vis spectrophotometer.

3. Results and Discussion

The X-ray diffraction patterns of the ZnO nanoparticles are shown in Figure 1. The diffraction patterns showed the highest peak indicating the different crystal orientation. The ZnO nanoparticle with pH 6 had the highest peak intensity at the plane (101), while the ZnO nanoparticles with pH 7 were at the plane of 002. The ZnO nanoparticle with pH 6 is in line with the result reported by Zhang *et al*. [16]. Meanwhile, the ZnO nanoparticle with pH 7 is in line with the study reported by Polsongkram *et al.*[17].

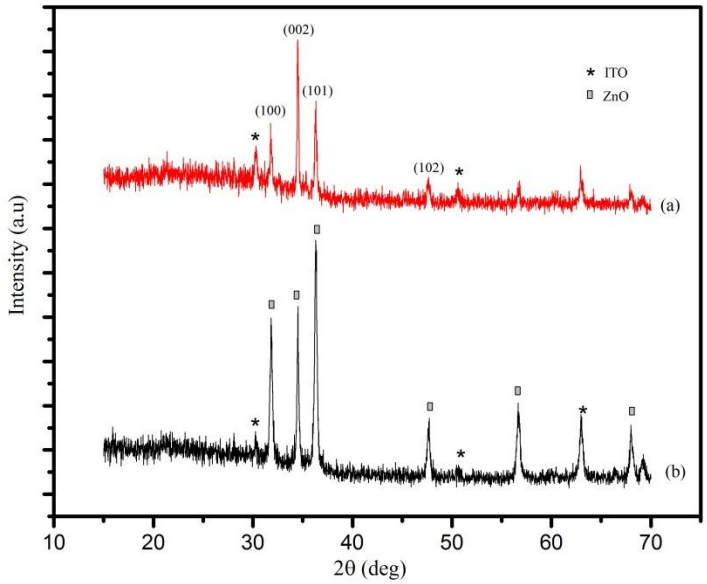

Figure 1. X-Ray Diffraction Patterns of The Zno Nanoparticles with Ph (a) 7 and (b) 6

In this work, the ZnO nanorods were synthesized by using the hydrothermal method with ZnO nanoparticles as a buffering layer in the concentrations of 30, 35, and 45 mM. The X-ray diffraction patterns are presented in Figure 2.

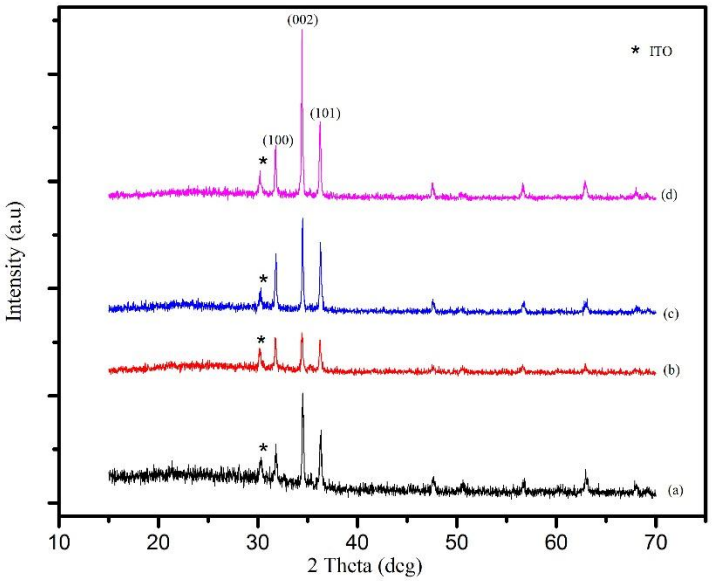

Figure 2. X-ray diffraction patterns of the ZnO nanorods with the precursor concentration on the buffering layer.

Figure 2 shows the X-ray diffraction pattern of ZnO nanoparticles and ZnO nanorods in various precursor concentrations. The three highest peaks were (100), (002), and (101). The crystal preferred orientation of the samples can be indicated by the highest peak intensity shown by Bragg plane of (002). It implied that the growth orientation was dominated by grains which were directed to (002) or perpendicular to the substrate. It is also obtained that the increase of precursor concentration caused the growth of the diffraction peak intensity. The highest peak intensity was obtained with the concentration of 45 mM. It could be inferred that the greater precursor concentration lead to be prefer of the crystal orientation of the ZnO nanorods to the c-axis at the (002) plane. Based on the Rietveld refinement method, the analysis results of the diffraction data are presented in Table 1.

Table 1. Refinement results of the samples

Parameter	ZnO Model	ZnO nanoparticles	ZnO nanorods 30 Mm	ZnO nanorods 35 mM	ZnO nanorods 45 mM
$a = b$ (Å)	3.2494	3.258	3.263	3.244	3.251
c (Å)	5.2038	5.213	5.224	5.193	5.206
c/a	1.6	1.6	1.6	1.6	1.6
V (Å^3)	-	47.5	48.17	47.35	47.65
GoF (%)	-	1.25	1.30	1.24	1.25
Rwp	-	19.29	33.89	31.01	32.31
Rp	-	15.11	25.81	23.52	23.76

Table 1 shows that the lattice parameter for all samples has a *c/a* ratio of about 1.60. It indicated that the structure of ZnO nanorods was formed in hexagonal wurtzite. Furthermore, the X-ray diffraction data was also analyzed by using Scherrer's equation to determine the particle size of ZnO nanorods. The calculation results are presented in Table 2.

Table 2. Particle size of the ZnO nanorods

Precursor Concentration (mM)	FWHM (rad)	Particle Size (nm)
30	0.20311	44.58
35	0.15385	58.87
45	0.1699	53.16

The particle size of the ZnO nanorods in the concentrations of 30, 35, and 45 mM were 44.58, 58.87, and 53.16 nm, respectively. We can see that the size increased from the concentration of 30 to 35 mM, and decreased from 35 to 45 mM. It was probably due to the effective reaction condition also provided by the sample with 35 mM. The temperature change at the period of growing can probably change the FWHM value and the average size of the crystal grain.

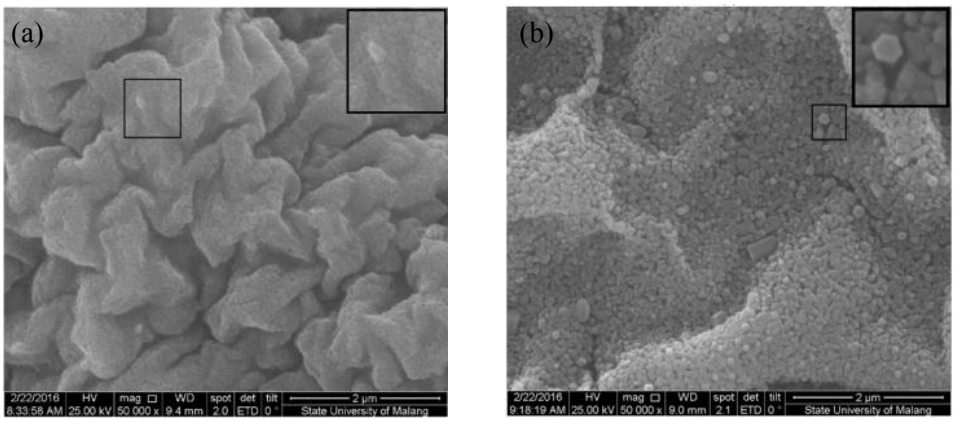

Figure 3. SEM images of ZnO films (a) pH 6; (b) pH 7

Based on Figure 3, we can see that the surface morphology showed a typical shape and size of ZnO. The figure also demonstrates that the sample obtained for pH 7 has a different morphology from pH 6. Furthermore, the SEM images of ZnO nanorods with the variation of precursor concentrations are displayed in Figure 4.

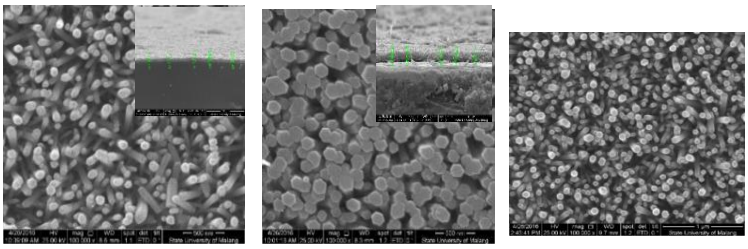

(a) (b) (c)

Figure 4. SEM images of the ZnO Nanorods with precursor concentrations of (a) 30 mM; (b) 35 mM; (c) 45 mM

Figure 4 showed that the results of synthesis presented that the ZnO nanorods has rod morphology with a hexagonal structure on the substrate surface. The particle size was analyzed and tabulated in Table 3. Meanwhile, further analysis results of average thickness of the films are listed in Table 4.

Table 3. Average diameter of the ZnO nanorods

Concentration (mM)	Diameter (nm)
30	94.21
35	156.3
45	76.68

Table 4. Average thickness of the ZnO Nanorods Films

Thickness	ZnO/ITO (µM)	ZnO Nanorods /ITO (µM)		
		30 mM	35 mM	45 mM
1	0.943	1.049	2.39	1.925
2	0.765	1.253	2.419	1.807
3	0.884	1.312	2.331	1.925
4	0.706	1.02	2.709	1.78
5	1.002	1.079	2.361	1.681
Average	**0.86**	**1.1426**	**2.442**	**1.8236**

Table 3 shows the diameters of the samples for the concentrations of 30, 35, and 45 mM that were 94.21, 156.3, and 76.68 nm, respectively. Theoretically, the nanorod is one of the nanostructures with the dimension length range of about 1-100 nm (Orhan, 2012). Therefore, in this work, the ZnO nanorods films that had the smallest size were the ones in the concentration of 35 mM.

The characterization of UV-Vis spectrophotometer was conducted to identify the absorbance and film transmittance of ZnO nanoparticles and nanorods. The wavelength used was in the range of 300-800 nm. The measurement results shown in Figure 5 presented that the absorbance value of the samples reduced along with the increasing wavelength. The ZnO nanorods absorption for all samples with different precursor concentrations was relatively similar. The figures show that the nanorods structure can enhance the light absorption. The absorbance value is in inverse with the transmittance, so the light passed along by the ZnO nanorods is less than the light passed along by the ZnO nanoparticles. The strongest excitonic absorption peak of all ZnO nanorods samples was located along the wavelength of ~375 nm, while the ZnO nanoparticles were located along the wavelength of ~350 nm. The wavelength was an emission peak of UV from free exciton.

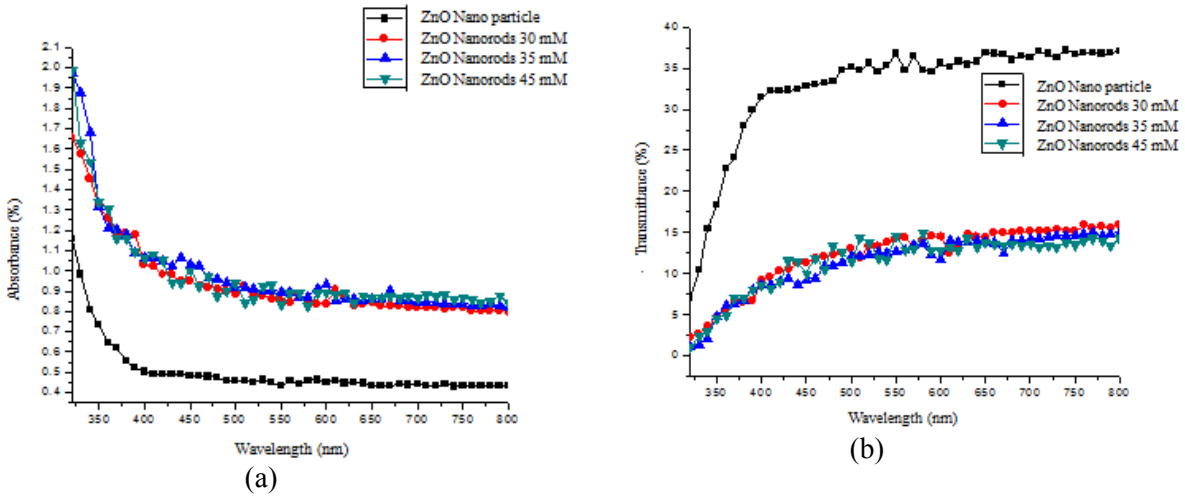

Figure 5. Result of UV-Vis Test on (a) Absorbance; (b) Transmittance

A band gap can be determined through the maximum and minimum transmittance values, film layer thickness, as well as the coefficient of thin layer absorption. The orientation of band gap is addressed through a position of graphic Tauc $(\alpha hv)^2$ versus. hv. This method was used to measure the difference between the valence band and the conduction band. The interceptions between the tangent to the linear portion of the curve and hv-axis in the ZnO nanoparticles film and the ZnO nanorods with

the variation of precursor concentrations are presented in Figure 6. The band gap of the samples is shown in Table 5.

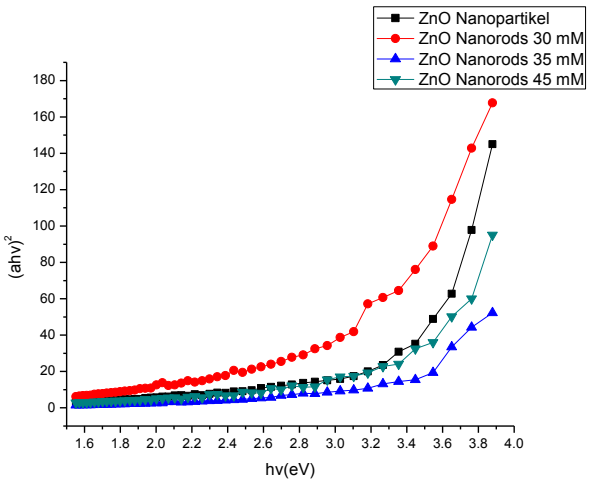

Figure 6. Tauc plot results of the ZnO nanoparticles and ZnO nanorods

Table 5. Band gaps of ZNO nanoparticles, and ZnO nanorods Films.

Sample	Band Gap (eV)
Film ZnO Nanoparticle/ITO	3.46 ± 0.99
Film ZnO Nanorods/ ITO 30 mM	3.14±0.99
Film ZnO Nanorods/ ITO 35 mM	3.16±0.98
Film ZnO Nanorods/ ITO 45 mM	3.18±0.96

From Table 5, it can be seen that the band gap of the ZnO nanoparticles film is ~3.46 eV. This result is in the range of the band gap of ZnO nanoparticles film which is 3.2-3.5 eV (Kasuma, 2012). The ZnO nanorods with the different precursor concentrations had a lower band gap than ZnO nanoparticles film. This phenomenon was originated from the ZnO nanorods that have a larger surface than that of ZnO nanoparticles. The ZnO nanorods can relatively increase the light absorption and lower the band gap of the material. The band gap of the ZnO nanorods for all samples with different precursor concentrations is relatively similar.

4. Conclusion

The crystal structure of the ZnO nanorods was hexagonal. The greater precursor concentration lead to grow the crystal orientation of the ZnO nanorods parallel to c-axis at the plane of (002). The particle size of the ZnO nanorods with the concentrations of 30, 35, and 45 mM, were 44.58 nm, 58.87 nm, and 53.16 nm, respectively. The greater the precursor concentration, the bigger rod diameter will be. The ZnO nanorods with the concentrations of 30, 35, and 45 mM had a relatively similar band gap, that was ~3.18 eV, while the band gap of the ZnO nanoparticles was ~3.46 eV.

5. References

[1] Sugiyono A *et al* 2014 *Outlook Energi Indonesia 2014* Jakarta: Pusat Teknologi Pengembangan Sumberdaya Energi (PTPSE).
[2] Jung H S and Nam G P 2015 Perovskite Solar Cells: From Materials to Devices **11**(1) 10-25
[3] Prakoso A B *et al* 2012 Optimasi Pembentukan Lapisan Boron P+ pada Permukaan Belakang Sel Surya untuk Peningkatan Efisiensi Sel Surya berbasis Wafer Silikon Monokristal. *TEKNOFISIKA*.**1**(1)
[4] Ozgur U *et al* 2005 A Comprehensive Review of ZnO Materials and Devices *J.Appl. Phys.* **98**(4) 1-103.
[5] Tsai K J *et al* 2012 n-ZnO nanorods/p^+-Si (111) heterojunction light emitting diodes *Nanoscale Research Letters* **7** (664) 1-6
[6] Chai G Y *et al* 2011 Fabrication and characterization of an individual ZnO microwire-based UV photodetector *Solid State Sciences* **13** 1205-1210
[7] Visimberga G E E *et al* 2010 Nanolaser from ZnO nanorods as natural resonance cavities *Phys. Status Solidi C7* **7**(6): 1668-1671
[8] Pawar A *et al* 2015 Growth of ZnO Nanorods using Hydrothermal for Gas Sensing Application *Research Journal of Physical Science* **3**(2): 1-3
[9] Loh L *et al* 2013 Perovskite Enhanced Solid State ZnO Solar Cells *Journal of Physics* **476**: 1-6
[10] Dhara S and Giri P K 2011 Enhanced UV photosensitivity from rapid thermal annealed vertically aligned ZnO nanowires *Nanoscale Research Letters* **6**:504
[11] Ding Y and Zhong L W 2009 Structures of planar defects in ZnO nanobelts and nanowires." Micron **40** (3): 335–42
[12] Foo K L *et al* 2014 Sol-Gel Synthesized Zinc Oxide Nanorods And Their Structural And Optical Investigation For Optoelectronic Application Malaysia *Nanoscale Research Letters*
[13] Mehrabian M and Aslyousefzadeh S 2015 Highly Efficient Hybrid Solar Cell Using ZnO Nanorods and Assessment of Changes in Cell Performance by Varying the Growth Period *Journal of The Korean Physical Society* **66** (10): 1527-1531
[14] Ibupoto Z H *et al* 2013 Hydrothermal Growth of Vertically Aligned ZnO Nanorods Using a Biocomposit Seed Layer of ZnO Nanoparticles *Materials* **6**: 3584-3597
[15] Kathalingam A, Park HC, Kim S D, Kim H S, Velumani S & Mahalingam T 2015 *Synthesis of ZnO nanorods using different precursor solution and their two terminal devices characterization* **26**:5724-5734
[16] Zhang X *et al* 2014 Effect of aspect ratio and surface defects on the photocatalytic activity of ZnO nanorods. *Scientific Reports*. **4**: 4596
[17] Polsongkram D *et al* 2008 Efeect Of Synthesis Conditions on the growth of ZnO nanorods via hydrothermal method *Physica B* **403**: 3713-3717

Acknowledgements
The authors would like to thank the KEMENRISTEKDIKTI RI, Mineral and Advanced Material Laboratory of Faculty of Mathematics and Natural Sciences, State University of Malang for the use of laboratory facilities.